1997 HST Calibration Workshop
Space Telescope Science Institute, 1997
S. Casertano, et al., eds.

The HST/FOS Wavelength Scale

Roeland P. van der Marel[1]

Space Telescope Science Institute, 3700 San Martin Drive, Baltimore, MD 21218

Abstract. I analyze the accuracy of the FOS pipeline wavelength calibration for the FOS/RD detector with the G570H grating. I use observations of arc spectra and external targets that I obtained in the context of studies of galactic nuclei, complemented with an observation of the planetary nebula NGC 6833 obtained by the FOS Instrument Science Team. The combined data were obtained in five visits spread over the period August 1995 to January 1997. I find that the absolute wavelength calibration generated by the pipeline for these visits is in error by 0.2–1.2 diodes, in the same direction for all visits. The mean of the errors is 0.62 diodes, where 1 diode = 4.37Å. The error is largest for the two visits that used the paired apertures. These results indicate that the grating-wheel non-repeatability is larger than believed, or that (some of) the dispersion solutions in the pipeline may need to be modified by a constant offset. There are variations in the S-distortion between visits at the level of ~ 0.1 diodes. The RMS shift between arc spectra obtained in the same visit, as a result of residual GIM errors, is $\lesssim 0.04$ diodes. The average internal/external offset determined from these data is consistent with the constant value that has been used by the pipeline since 1992. No dependence is found on aperture or epoch. However, there is an indication that the internal/external offset varies systematically by 0.15 diodes between the blue and the red ends of the grating. If true, this translates directly into a systematic error in the relative wavelength scale for all G570H FOS/RD data in the HST Data Archive.

1. Introduction

The FOS pipeline calibration assigns a wavelength λ to each pixel x in a spectrum. The dispersion relations $\lambda(x)$ for all detector/grating combinations were determined from an analysis of internal arc lamp spectra. The underlying principle is that the dispersion relation must place the centroid of each arc emission line at its known vacuum wavelength, plus an offset. The offset accounts for the fact that the light from the internal arc lamps traverses a different path in the instrument than the light from an external target. This offset is conventionally expressed as $X_{\rm off} \equiv X_{\rm internal} - X_{\rm external}$ in detector diodes; I will refer to it as the internal/external offset. This quantity must itself be calibrated, which can be done from observations of any target with known radial velocity. Kriss, Blair & Davidsen (1992) used pre-COSTAR observations of an M star with strong emission lines, obtained in September 1991. They found $X_{\rm off} = +0.176$ diodes for FOS/RD and $X_{\rm off} = -0.102$ diodes for FOS/BL, in either case with only a small dependence ($\lesssim 0.05$ diodes) on the choice of grating. The observations were done with the 0.3 aperture, and a possible dependence on the choice of aperture was not tested for. These internal/external offsets have been used in the pipeline since 1992, and have not been updated after the installation of COSTAR.

[1]STScI Fellow

visit	#	date	galaxy	aperture(s)	D diodes	RMS(d_j) diodes	$X_{\rm off}$ diodes
5847/1	9	08/22/95	M32	0.1/0.25	1.40	0.03	0.16 ± 0.02
5848/2	7	09/07/95	NGC 7052	0.3	0.38	0.03	0.19 ± 0.10
5848/4	7	08/17/96	NGC 7052	0.3	0.42	0.02	0.19 ± 0.10
6537/2	6	11/30/96	IC 1459	0.1/0.25	1.02	0.04	0.49 ± 0.30

Table 1. The first five columns list the project-ID/visit-number, number of orbits in the visit, date of the observations, name of the galaxy that was studied, and aperture(s) that was (were) used; '0.1/0.25' refers to the upper paired apertures of the given size. The next two columns list characteristics of the wavelength scale. The quantity D is the offset between the inferred wavelength scale for the visit, and the wavelength scale generated by the pipeline; RMS(d_j) is the RMS shift in the wavelength scale during the visit as a result of residual GIM errors. The last column lists the estimate of the internal/external offset $X_{\rm off}$ for the FOS/RD detector with the G570H grating, obtained from the galaxy spectra as discussed in Section 3; the two NGC 7052 visits were combined to yield a single estimate.

The accuracy of the FOS wavelength scale provided by the pipeline is limited by several effects (see, e.g., Keyes et al. 1995). **(1)** Non-repeatability in the positioning of the filter-grating wheel. Koratkar & Martin (1995) measured maximum deviations of ~ 0.35 diodes, more-or-less independent of the choice of either the grating or the detector; the RMS deviation was ~ 0.1 diodes. Grating wheel non-repeatability is believed to be the dominant uncertainty in the pipeline wavelength scale. However, it can be fully corrected in projects where arc lamp spectra were obtained in addition to the spectra of external targets, with no grating wheel motion in between. **(2)** Target acquisition uncertainties. The centering of the target in the aperture affects the accuracy of the wavelength scale. Errors are minimized by the choice of an accurate acquisition strategy, and can be corrected post-hoc if the position of the target in the aperture is known, e.g., from an FOS/ACQ image taken in the same orbit. **(3)** Residual errors in the on-board correction for the geomagnetically induced image motion problem (GIM). These have not been reported to exceed 0.1 diodes (HST Data Handbook 1995). Residual GIM errors can be corrected if the spectra of the external target are interspersed with frequent arc lamp spectra. **(4)** Errors in the internal/external offset. The measurements by Kriss et al. (1992) had a 1σ uncertainty of 0.1 diodes. The offset may also depend on epoch, or may have changed with the installation of COSTAR. **(5)** Uncertainties in the dispersion solutions. The dispersion solution to an arc spectrum generally fits individual lines with a RMS of 0.01–0.08 diodes, depending on the choice of grating (HST Data Handbook 1995). The dispersion solutions may also depend on epoch.

In the context of the Cycle 5 and Cycle 6 projects GO-5847, 5848 and 6537, I analyzed FOS/RD spectra with the G570H grating of the nuclear regions of the galaxies M32, NGC 7052 and IC 1459 (see Table 1). The goal of these projects was to infer the nuclear mass distribution from the observed stellar and/or gas kinematics, and to determine the mass of possible black holes. The spectra for GO-5847 and 6537 were obtained in one visit each (5847/1 and 6537/2), while the spectra for GO-5848 were obtained in two visits (5848/2 and 5848/4), separated by one year. The first two orbits in each visit were used for target acquisition. There were no grating-wheel motions after the acquisition. In each orbit, arc lamp spectra were obtained during occultation to allow the construction of an optimally accurate wavelength scale. The galaxies have known systemic velocities, and the FOS/RD G570H internal/external offset could therefore be measured from the data. The scientific results from these projects are discussed elsewhere (van der Marel, de Zeeuw & Rix 1997; van der Marel & van den Bosch 1998; van der Marel, Carollo et al. 1998). Here I use the data to study the accuracy of the FOS pipeline wavelength scale.

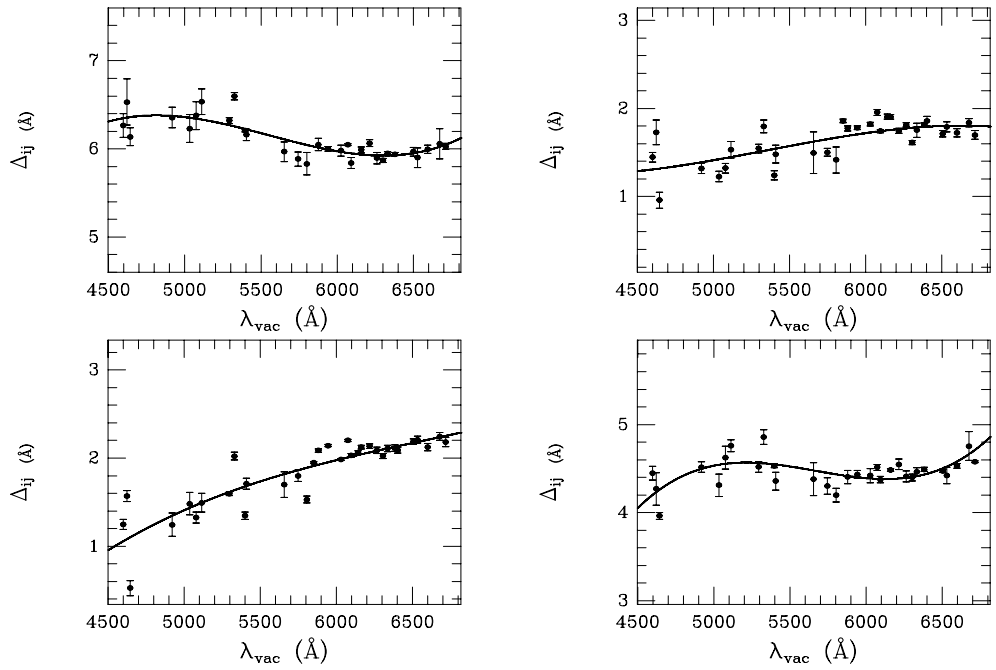

Figure 1. Wavelength calibration results for 5847/1 and 5848/2 (top row) and 5848/4 and 6537/2 (bottom row). Data points show for each arc emission line i at wavelength $\lambda_{\mathrm{vac},i}$ (plotted along the abscissa), the mean Δ_{ij} averaged over the arc spectra j in the given visit; the quantity Δ_{ij} is the difference between the vacuum wavelength, and the central wavelength of the line measured on the wavelength scale provided by the pipeline. The scale along both axes is in Å. The size of each panel along the ordinate is the same, but the range of displayed values is different. The curve in each panel is the best-fitting third order polynomial $(D + P_3(\lambda_{\mathrm{vac},i}))$. Arc lines at larger wavelengths have higher signal-to-noise ratio, and their centroids therefore have smaller errors.

2. Wavelength calibration

I wrote fortran software to perform the wavelength calibration for these projects. The centroids of non-blended lines in the arc lamp spectra were determined through Gaussian fits. This yields for each spectrum j, and for each line i with vacuum wavelength $\lambda_{\mathrm{vac},i}$, the observed wavelength λ_{ij} on the scale provided by the pipeline. For each visit I fitted the observed offsets $\Delta_{ij} \equiv \lambda_{\mathrm{vac},i} - \lambda_{ij}$ as

$$\Delta_{ij} = D + d_j + P_3(\lambda_{\mathrm{vac},i}). \tag{1}$$

The quantity D is a constant offset. It is expected to be equal to +0.176 diodes (the internal/external offset in the pipeline; by convention, the pipeline scale is tailored to be correct for external targets, and hence to be offset for the internal lamps), plus an unknown offset that is different for each visit, due to grating wheel non-repeatability. The d_j represent shifts of the wavelength scale between arc spectra within the same visit (i.e., on a time scale of orbits), and are expected to be non-zero due to residual GIM errors. The third order polynomial P_3 (with zero mean, by convention) accounts for differences between the actual S-distortion of the wavelength scale, and that part of the S-distortion that is already corrected by the pipeline.

Table 1 lists D and the RMS of the d_j for each visit, expressed in diodes (1 diode = 4.37Å for the G570H grating). Figure 1 shows the results as function of wavelength,

averaged over the multiple arc spectra in a given visit. The shifts in the wavelength scale during a visit as a result of residual GIM errors are small, RMS(d_j) $\lesssim 0.04$ diodes. The residual S-distortion varies from visit to visit, but is also small, $|P_3| \lesssim 0.1$ diodes. The inferred values of D are surprising. They are not randomly distributed around +0.176 diodes, as would have been expected. Instead, $D - 0.176$ ranges from 0.2–1.2 diodes, and has the same sign for all visits. The error is particularly large for the two visits that used the upper paired apertures. These results indicate that the grating-wheel non-repeatability is larger than believed, or that (some of) the dispersion solutions in the pipeline may need to be modified by a constant offset. The quantities $D-0.176$ provide a direct comparison between the dispersion solutions from my data and the dispersion solutions used by the pipeline. Both are based on arc spectra, and the inferred discrepancy is therefore independent of the internal/external offset.

3. The internal/external offset

I used the dispersion solutions for the arc spectra to generate an optimal wavelength scale for each of the galaxy spectra in each visit, initially assuming that there is no internal/external offset. Residual GIM errors were corrected by shifting the wavelength scale for each galaxy spectrum by the (small) amount d_j determined for the arc spectrum (spectra) obtained in the same orbit. The absorption and/or emission lines in the galaxy spectra were analyzed to determine the mean velocities of the stellar and/or gaseous components. The distribution of light within the aperture was modeled for each observation, and the small velocity shifts resulting from a possible asymmetric distribution of light within the aperture were corrected for. Rotation curves were generated using the results from spectra obtained at various distances along the major axis, and the mean velocity at the position of the nucleus (obtained by interpolation) was adopted as the inferred systemic velocity. The systemic velocity for each galaxy was compared to literature values available from ground-based observations. The difference $\Delta V \equiv V_{\rm obs} - V_{\rm lit}$ provides a measurement of the internal/external offset. For the FOS/RD with the G570H grating, $X_{\rm off} = (\Delta V/c) \times (\lambda_{\rm obs}/4.37\text{Å})$, where c is the speed of light and $\lambda_{\rm obs}$ is the wavelength (or the mean of the wavelength region) used to derive the velocity.

For M32 only absorption lines are available. However, the spectra have very high signal-to-noise ratio, and the apertures sampled the nuclear region densely. The systemic velocity and the internal/external offset are therefore accurately determined. The result, $X_{\rm off} = 0.16 \pm 0.02$ is entirely consistent with the value of 0.176 diodes (with a quoted 1σ error of ~ 0.1 diodes; Kriss et al. 1992) that has been used for years by the pipeline. The NGC 7052 and IC 1459 observations were aimed at a determination of the gas kinematics; the absorption lines have too little signal for an accurate determination of $X_{\rm off}$. The emission lines have sufficient signal, but their kinematics are more difficult to interpret. The gas near the nucleus need not move at the systemic velocity, and the presence of dust in both galaxies provides additional uncertainties. For IC 1459 there are also differences of up to 100 km/s in the systemic velocities quoted in the literature. The errors in $X_{\rm off}$ listed in Table 1 for NGC 7052 and IC 1459 provide my assessment of the possible importance of these complicating factors, based on extensive tests. The $X_{\rm off}$ determinations for these galaxies are less accurate than for M32, but as for M32, the results are consistent with the internal/external offset that is used by the pipeline.

4. Analysis of a planetary nebula spectrum

Galaxies are not the most convenient targets to determine the internal/external offset of the FOS. Planetary nebulae are more suitable, because of their pronounced emission lines and lack of intrinsic kinematic gradients. The FOS instrument team has observed the planetary

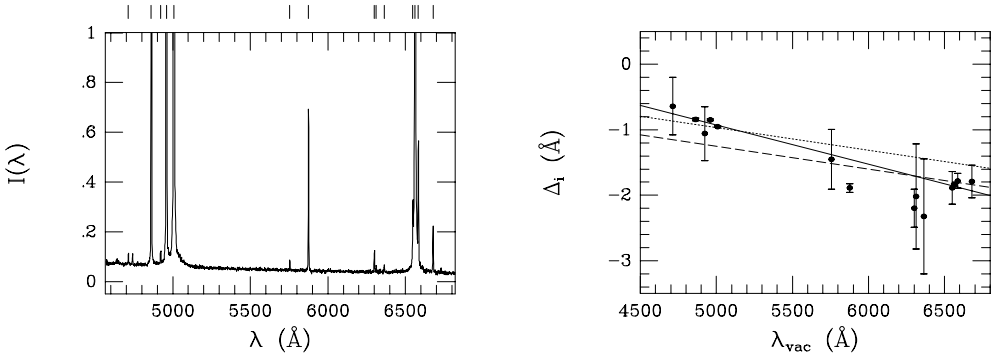

Figure 2. The left panel shows a spectrum of the planetary nebula NGC 6833. Bars indicate the emission lines that were identified and fitted: HI ($\lambda_{\rm air} = 4861.33$, 6562.82Å), He I (4713.20, 4921.93, 5875.67, 6678.15), [OI] (6300.30, 6363.78), [NII] (5754.64, 6548.03, 6583.41), [OIII] (4958.91, 5006.84) and [SIII] (6312.10). The vacuum wavelengths follow from $\lambda_{\rm vac} = \lambda_{\rm air}\, n_{\rm air}$, where the index of refraction for air $n_{\rm air} \approx 1.000279$. The right panel shows the residuals Δ_i between the measured and the vacuum wavelength of the emission lines, as a function of $\lambda_{\rm vac}$. The scale along the ordinate is in Å. These data allow an accurate determination of the internal/external wavelength offset. The linear fits are discussed in the text.

nebula NGC 6833 as part of its calibration program. To verify the results reported in Sections 2 and 3, I analyzed a spectrum (y3kk010ct) of NGC 6833 and a contiguous arc spectrum (y3kk010dt), obtained on 01/12/97 with the 0.3 aperture and G570H grating on the FOS/RD detector. These spectra were taken as part of proposal 6918 (PI: Keyes), and were kindly provided to me by E. Smith. These and more spectra of the same target are also available from the HST Data Archive.

The arc spectrum was analyzed as described in Section 2. The offset D was found to be 0.76 diodes; as before, significantly larger than the expected value of 0.176 diodes, and too large to be attributable to grating wheel non-repeatability. The wavelength solution for the arc spectrum was used to calibrate the NGC 6833 spectrum, initially assuming that there is no internal/external offset. The spectrum is shown in the left panel of Figure 2. Gaussians were fitted to all detectable emission lines (indicated in the Figure and listed in the caption), yielding for each line i the observed wavelength λ_i. The right panel of the figure shows the inferred residuals $\Delta_i \equiv \lambda_i - \lambda_{{\rm vac},i}$ as a function of $\lambda_{\rm vac}$.

The observed and vacuum wavelength for a line are related according to

$$\Delta = 4.37\, X_{\rm off} + (V/c)\lambda_{\rm vac}, \tag{2}$$

where V is the line-of-sight velocity of NGC 6833 with respect to the earth at the time of the observation, and 4.37 is the scale in Å/diode for the G570H grating on the FOS/RD detector. This is a linear relation between Δ and $\lambda_{\rm vac}$; the velocity V determines the slope, and the internal/external offset determines the intercept. The heliocentric velocity of NGC 6833 from the literature is -109.8 km/s. This implies $V = -104.0$ km/s, taking into account the annual velocity of the earth as calculated with the IRAF task `rvcorrect`. The dotted line in Figure 2 shows the best fit line for this velocity when the individual Δ_i are weighted by their errors. The inferred internal/external offset, $X_{\rm off} = 0.177$, is then determined primarily by the three strong lines near 5000Å. The dashed line shows the fit if the Δ_i are all weighted equally, which yields $X_{\rm off} = 0.111$ diodes. These results are in satisfactory agreement with both the pipeline value and the results of Section 3, indicating that there is no appreciable dependence of $X_{\rm off}$ on either epoch or aperture.

Neither the dotted nor the dashed line in Figure 2 fits the data on both the blue *and* the red ends of the spectrum. If one assumes that this is due to an error in the literature

value for the heliocentric velocity, one must also assume that the internal/external offset in the pipeline (and verified in Section 3) is wrong. This is not a plausible explanation. It is more likely that the internal/external offset is not a pure constant, but is of the form $X_{\rm off} = A + BX$. This still yields a linear relation between Δ and $\lambda_{\rm vac}$, but now of the form

$$\Delta = [-sA + B(\lambda_1 - s)] + [(V/c) - B]\lambda_{\rm vac}, \tag{3}$$

where λ_1 is the wavelength at the first diode. The solid line in Figure 2 shows the best linear least squares fit of this form, when the Δ_i are weighted by their errors. It has $A = 0.080$ and $B = 2.53 \times 10^{-4}$. A similar fit, but with all data weighted equally, yields $A = 0.036$ and $B = 3.24 \times 10^{-4}$. The internal/external offset at the first diode (on the red end) is $A + B \approx A$. At the last diode (number N; on the blue end), it is $A + NB = 0.210$ or 0.202, depending on whether the data points are weighted in the fit or not. Thus, it appears that the internal/external offset varies from $X_{\rm off} \approx 0.21$ diodes on the blue end to $\rm X_{off} \approx 0.06$ diodes on the red end. The addition of a linear term in $X_{\rm off}$ decreases the χ^2 of the fit from 438 to 70 (for 12 degrees of freedom), and is thus highly significant. The relatively low values of the Δ_i for the emission lines in the range 5800–6500Å may indicate that even second- or higher-order terms should be invoked for an accurate description of the internal/external offset.

5. Conclusions

The results presented here show that the pipeline wavelength calibration for the FOS/RD detector with the G570H grating is somewhat less accurate than has been believed. The results of Section 2 suggest that there are errors in the *absolute* scale that are both systematic and surprisingly large, and that can therefore not be attributed to the usual grating wheel non-repeatability. The results of Section 4 show that the internal/external offset may not be a simple constant, but may have a systematic variation of ~ 0.15 diodes between the two sides of the detector. If so, this translates directly into a systematic error in the *relative* wavelength scale for all G570H FOS/RD data in the HST Data Archive. Improvements in the pipeline calibration parameters may be feasible, and should be followed by a recalibration of all impacted data in the Archive.

Acknowledgments. This work benefited from discussions with FOS Instrument Scientists Tony Keyes and Ed Smith. They are currently studying the FOS wavelength calibration in a more systematic fashion, and kindly shared with me both their data (on NGC 6833) and their insights. The FOS spectra of M32, NGC 7052 and IC 1459 were obtained in collaborations with Tim de Zeeuw, Hans-Walter Rix, Frank van den Bosch, Marcella Carollo and Marijn Franx.

References

Keyes C. D., Koratkar A. P., Dahlem M., Hayes J., Christensen J., Martin S. 1995, *FOS Instrument Handbook*, Version 6.0, (Baltimore:STScI)

Koratkar A., Martin S. 1995, Instrument Science Report CAL/FOS-145 (Baltimore:STScI)

Kriss G.A., Blair W.P., Davidsen A.F. 1992, Instrument Science Report CAL/FOS-070 (Baltimore:STScI)

van der Marel R. P., de Zeeuw P. T., Rix H.-W. 1997, ApJ, 488, in press

van der Marel R. P., van den Bosch F. C. 1998, in preparation

van der Marel R. P., Carollo C. M. C., de Zeeuw P. T., Franx M. 1998, in preparation